Calcif Tissue Int (2003) 73:49–55
DOI: 10.1007/s00223-002-2120-4

Calcified Tissue International

Laboratory Investigations

Establishment of a Model of Cortical Bone Repair in Mice

T. M. Campbell, W. T. Wong, E. J. Mackie

School of Veterinary Science, University of Melbourne, Parkville, Victoria 3010, Australia

Received: 20 August 2002 / Accepted: 5 December 2002 / Online publication: 8 April 2003

Abstract. A model of cortical bone repair has been established for use in mice. The cortical defect consisted of a hole drilled through the entire diameter of the tibial diaphysis. The hematoma that initially filled the drill site was invaded by cells of mesenchymal appearance within 5 days of injury. Trabeculae of mineralized woven bone were present throughout the drill site by day 9. A reaction in the periosteum adjacent to the drill site, consisting of both new bone and cartilage formation, preceded deposition of bone tissue in the drill site. New woven bone was modeled to restore the marrow cavity to normal by 4 weeks after injury, and almost normal cortical structure was achieved by 6 weeks after injury. Immunohistochemical studies indicated that type III collagen was expressed within the drill site by day 5, reached a peak at day 7, and was diminished by day 9. In contrast, type I collagen was first detectable in the drill site at day 7, and staining was more intense by day 9. Osteopontin expression in the drill site coincided with the process of mineralization of new bone in this location. The model of bone repair described here provides a method for inducing reproducible bone lesions in a readily identifiable location in mice. It will be useful in the investigation of bone cell function in mouse strains that have been subjected to genetic manipulation.

Key words: Osteoblast — Osteoclast — Bone repair — Collagen — Osteopontin

The availability of genetically modified mice in recent years has led to a demand for mouse models of pathological conditions in which the roles of specific gene products can be investigated. In many cases, genetically manipulated mice have shown surprisingly normal phenotypes during development and growth, but responded abnormally when subjected to pathological interventions [1–3].

Bone repair is a process involving several cell types undergoing accelerated activity in a variety of biological processes with a specific sequence. For example, osteoblast precursors undergo migration, proliferation and differentiation before laying down the osteoid necessary for new bone formation. Osteoclasts, blood vessels, bone marrow cells and chondrocytes are also involved to varying degrees, depending on the nature of the injury. Thus, bone repair represents a useful set of events through which to investigate the role of proteins expressed in bone in regulating cellular activity.

Experimental models of bone repair have been developed for a variety of purposes, including the investigation of factors influencing fracture repair, and development of improved methods of managing fractures in humans and animals. The majority of these models have made use of the larger experimental animal species such as rabbits and sheep. Mice have been used infrequently; they are too small to provide a useful model of fracture repair where biomechanical conditions similar to those in humans are required, and because of their size it is technically difficult to obtain reproducible fractures in this species. Previously published models of bone repair in mice include a model involving an unstabilized fracture 4] and others involving a fracture stabilized by internal [5] or external fixation [6, 7].

We were interested in investigating the process of bone repair in a particular genetically manipulated ('knockout') mouse strain, and undertook some preliminary studies using an internally fixed fracture of the tibia, as described by Hiltunen et al. [5]. We observed that there were large differences between individuals in the nature of the fracture produced, and concluded that this method was inappropriate for our purposes, since we expected that differences between knockout and wildtype mice may be subtle. The aim of this work was to develop a means of investigating bone repair in mice that could be used in genetically manipulated mouse strains to investigate the role of specific proteins in bone cell function. The following criteria were considered important for achieving such an outcome: the method should be technically relatively simple; it should not lead to distress in the animals; the defect should be produced in a readily identifiable anatomical location; and the defect should be

Correspondence to: E. J. Mackie; E-mail: ejmackie@unimelb.edu.au

highly reproducible. The current paper describes the characterization of a method of investigating bone repair in mice that satisfies all of these criteria.

Materials and Methods

Animals and Surgery

Male 129/Sv mice were bred at the School of Veterinary Science Animal House and subjected to surgery at 12–14 weeks of age. All work involving animals was approved by the Animal Experimentation Ethics Committee of the School of Veterinary Science and was in compliance with the Guiding Principles in the Care and Use of Animals endorsed by the American Physiological Society. Mice were anesthetized, then a skin incision was made over the medial aspect of the proximal end of the tibia. Soft tissue was cleared away and a single hole (500 μm diameter) was drilled through the tibia with a 25-gauge needle in a cordless drill. The hole was drilled at the level of the distal end of the tibial crest through the entire diameter of the tibia, i.e., through medial and lateral cortices and the intervening medulla. The skin was sutured closed following drilling. The same procedure was then carried out on the opposite leg. The mice were examined daily for any abnormal behavior, weight loss or diminished feed intake, but none of these was observed. Mice were randomly allocated to groups (n = 5) and euthanased at 3, 5, 7, 9, 14, 28, and 42 days postoperatively.

Histology

Tibiae were excised with some surrounding soft tissue. Right tibiae were processed for embedding in plastic, and left tibiae were processed for preparation of cryosections. For plastic embedding, tissues were fixed in 70% ethanol. Some tissues were then demineralized in 0.33 M EDTA (pH 7.4), whereas others were processed undemineralized. Tissues were embedded in LR White-Hard (London Resin Company, Reading, UK) according to the manufacturer's instructions. Transverse sections (5 μm) were cut using a slab microtome with a tungsten knife. Sections of undemineralized bone were fixed to slides using double-sided adhesive tape. Demineralized sections were stained with Masson's trichrome stain, and undemineralized sections were stained with von Kossa and counterstained with toluidine blue and basic fuchsin.

Cryosections were prepared as described [8]. Briefly, left tibiae were fixed in 4% paraformaldehyde in phosphate-buffered saline (PBS) for 90 min, then washed in PBS and incubated in 0.33 M EDTA (pH 7.4) at 4°C until demineralized. Bones were incubated overnight in 25% sucrose in PBS then embedded in OCT compound, frozen rapidly in liquid nitrogen, and stored at −80°C. Sections (10 μm) were cut in a freezing microtome, placed on slides coated with 3-aminopropyltriethoxysilane (Sigma) and stored at −80°C. Sections were stained for the presence of tartrate-resistant acid phosphatase (TRAP) to assist in the identification of osteoclasts; sections were incubated in 0.1 M sodium acetate buffer (pH 5.2) containing naphthol AS-TR phosphate (0.7 mg/ml) and fast red TR salt (0.7 mg/ml) in the presence of 10 mM sodium tartrate for 5 min at 37°C, then counterstained with hematoxylin and mounted with Aquamount (BDH). Sections used for immunohistochemistry were incubated with bovine testicular hyaluronidase (Sigma; 500 U/ml in 0.15 M NaCl, 0.02 M sodium acetate, pH 5.0, 30 min at room temperature). Slides were washed in PBS, incubated in 1% hydrogen peroxide in methanol for 20 min, then washed again in PBS. Sections were blocked in normal sheep serum (5% in PBS) then incubated overnight with primary antibody diluted in PBS containing 5% sheep serum. Rabbit anti-collagen type I, kindly provided by Drs J. Bateman and S. Lamandé (Department of Pediatrics, University of Melbourne), was prepared against a synthetic peptide corresponding to the mouse collagen α2(I) N-telopeptide, and was used at a dilution of 1:4,000. Rabbit anti-rat collagen type III (Chemicon, Temecula, CA, USA) was used at 1:1,000. Rabbit anti-human osteopontin (LF-123; kindly provided by Dr L.W. Fisher, NIH, Bethesda, MD, USA) was used at 1:2,000. Normal rabbit serum at the appropriate dilution was used as control. Primary antibodies were detected by the avidin-biotin-peroxidase complex procedure (Immunopure ABC peroxidase staining kit, Pierce) and diaminobenzidine (tablets from Sigma), according to the manufacturers' instructions. Sections were mounted with Aquamount. Background staining with normal rabbit serum is only shown at the dilution appropriate for osteopontin (1:2,000) (Fig. 5B), but similar levels of backgound were obtained for collagen type I and III staining.

Results

Morphological Observations

Following surgery, the mice recovered from anesthesia and started moving normally around their cages. They appeared to tolerate the procedure extremely well. Drill sites were visible grossly as a reddened area in excised tibiae in animals killed up to 7 days after drilling. The site of the lesion could still be identified until day 14 as a result of the adjacent soft tissue reaction, but was no longer visible from day 28.

The process of bone repair following drilling was examined microscopically in transverse sections through the drill site. Low power images of an undrilled tibia at the site of drilling, as well as drill sites from animals killed at various stages up to day 42, are shown in Figure 1.

Three days after drilling, it could be seen that a cylinder of tissue consisting of medial and lateral cortices and the intervening bone marrow had been removed by the drill and replaced by a hematoma (Fig. 1B). Very few cells were visible within the drill site, and those that were present appeared morphologically to be white blood cells. Bone chips resulting from the drilling were visible within the marrow cavity adjacent to the drill site, as well as in the muscle mass on the lateral side of the tibia. By day 5, numerous cells had appeared in the drill site but no mineralized matrix was visible within the drill site in sections stained with von Kossa; some periosteal new bone growth was seen adjacent to the drill site (Fig. 2A). By day 7, the drill site tissue had become denser, with a fibrillar extracellular matrix interspersed among cells of mesenchymal appearance (Figs. 1C, 3A). New bone formation on periosteal surfaces adjacent to the drill site was more advanced, and some cartilaginous tissue was visible in this region (Figs. 1C, 3B). In von Kossa-stained sections, small islands of mineralized matrix were present in the drill site (not shown).

The drill site was filled with new bone tissue by day 9. This tissue consisted of spicules of woven bone lined by osteoblasts, with spaces between spicules containing loosely arranged stromal and hemopoietic cells (Fig. 3C).

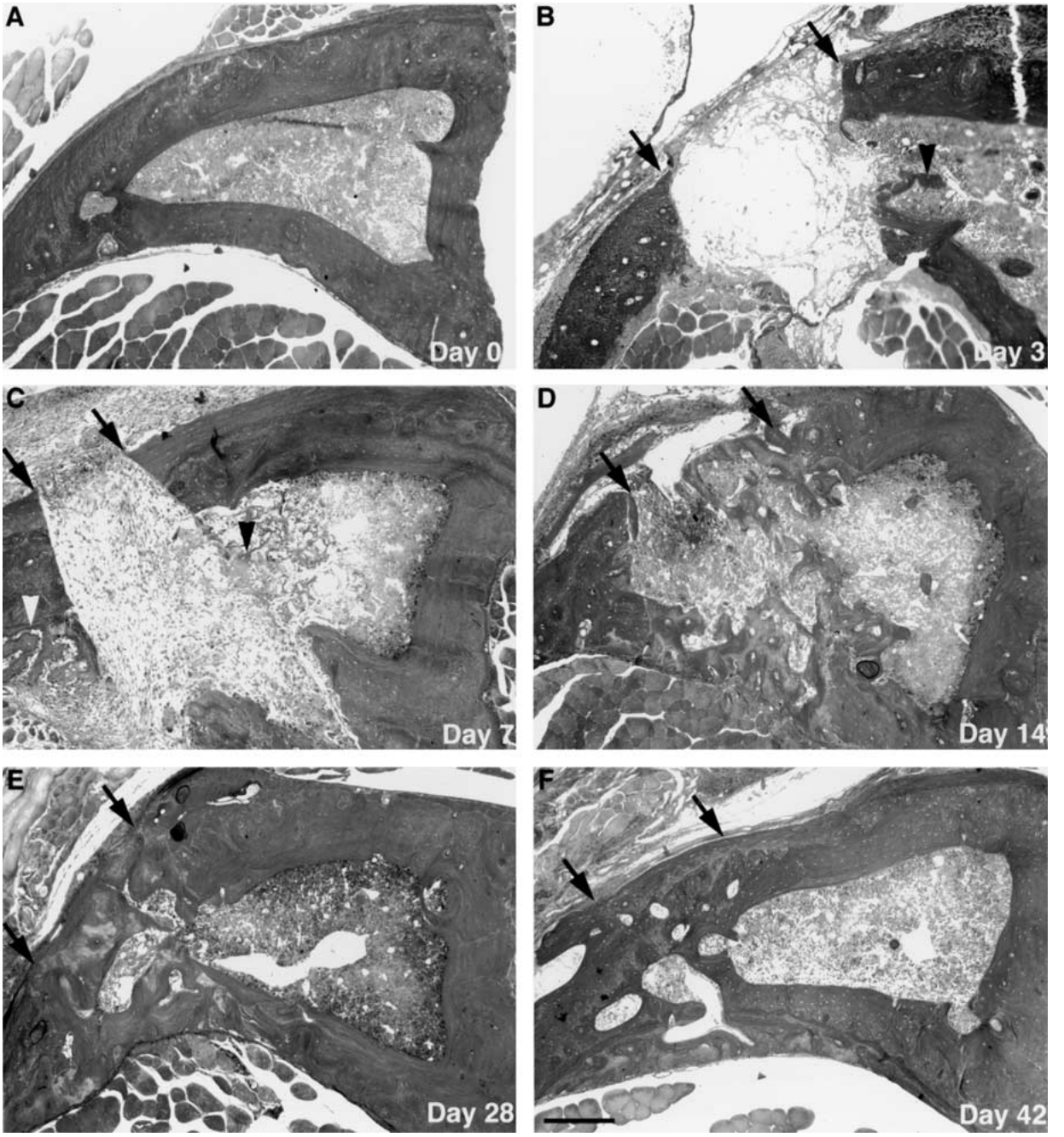

Fig. 1. Repair of cortical defect of tibia. Transverse sections of a normal mouse tibia (**A**) day 0 and of mouse tibiae 3, 7, 14, 28, and 42 days after drilling (**B**–**F**). Arrows indicate the edges of the drill site in the medial cortex; black arrowheads indicate bone chips left in the marrow cavity as a result of drilling; white arrowhead (**C**) indicates periosteal new bone formation. Demineralized plastic sections stained with Masson's trichrome. Bar (**F**) represents 200 μm; magnification the same for all figure parts.

Sections stained with von Kossa demonstrated that new bone within the drill site was well mineralized at day 9 (Fig. 2B). Some osteoclasts had appeared within the drill site at this stage, indicating that the new bone was beginning to be modeled (Fig. 3D). Further modeling was apparent at day 14. Some of the trabecular bone occupying the region of the drill site within the marrow cavity had been removed, whereas the trabeculae within the cortical bone defect had become thicker (Figs. 1D, 3E); osteoclasts were now abundant in the drill site (Fig. 3F). Spaces between trabeculae contained dense hemopoietic tissue with the appearance of normal bone marrow (Figs. 1D, 3E).

Four weeks after drilling (day 28), the cortical defect had been largely filled in through deposition of lamellar bone on the woven bone trabeculae (Fig. 1E). Some

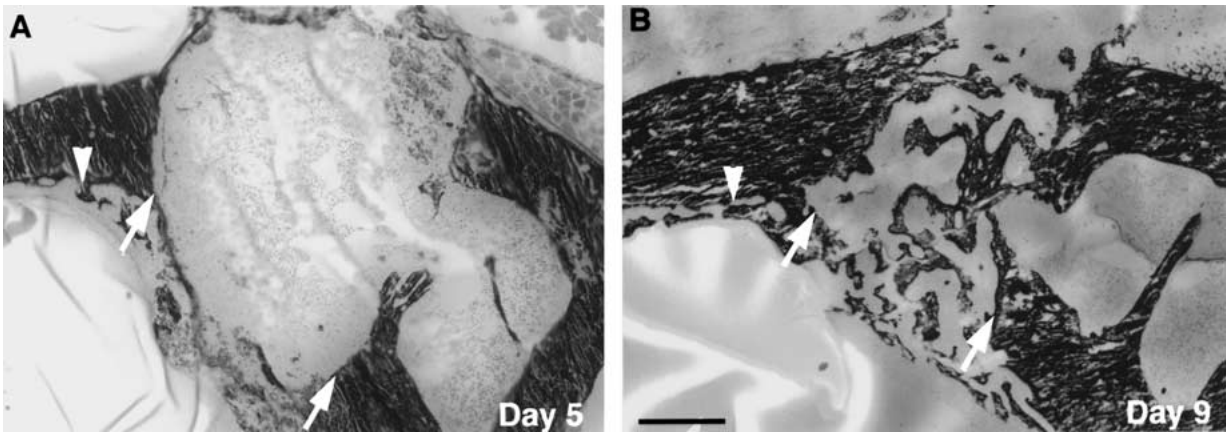

Fig. 2. Mineralization of the drill site. Transverse sections of mouse tibiae 5 (**A**) and 9 days (**B**) after drilling. Arrows indicate the edges of the drill site in the lateral cortex, and arrowheads indicate new bone formation in the periosteum adjacent to the drill site. Undemineralized plastic sections stained with von Kossa and epoxy stain. Bar = 200 μm.

excessive bone remained within the marrow cavity and on periosteal surfaces adjacent to the drill site. By day 42, the drill site could only be identified by the presence of some remaining woven bone and increased porosity within the cortex (Fig. 1F).

Immunohistochemistry

The patterns of expression of two important bone extracellular matrix proteins, collagen type I and osteopontin, as well as that of a protein associated with tissue repair, collagen type III, were investigated by immunohistochemistry in the repairing drill site. Collagen type III was undetectable in cortical bone adjacent to the drill site, but was weakly detectable within the drill site at day 5 (Fig. 4B). Expression of collagen type III reached a maximum at day 7, and was becoming weaker by day 9 (Fig. 4D, F). In contrast, collagen type I was present in undamaged cortical bone and bone chips adjacent to the drill site, but was absent from the tissue filling the drill site at day 5 (Fig. 4A). Collagen type I was detectable in a fibrillar distribution throughout the drill site at day 7 (Fig. 4C). At day 9, collagen type I staining was strong, but restricted to the bone trabeculae, where it was almost homogeneously distributed in the matrix (Fig. 4E). Osteopontin staining was strong in undamaged bone and bone chips at all time points, but first appeared in the drill site in scattered islands at day 7 (Fig. 5). By day 9, strong staining for osteopontin was present in a fibrillar distribution throughout the new bone filling the drill site (Fig. 5D).

Discussion

Here we describe a new method for experimental investigation of bone repair in mice. The method proved to be relatively simple to perform and was well tolerated by the animals. From the point of view of animal welfare, the method is clearly preferable to the fracture methods previously described in mice. The fact that the defect does not involve bone fracture not only ensures that it is less painful but also means that it can be applied bilaterally, thus providing more material per animal and the possibility of reducing animal numbers. The method provided much more reproducible lesions than the internally stabilized fracture method previously attempted in our laboratory; this will allow the use of fewer animals for the observation of differences between treatment groups. The drilling method is easier and can be carried out more rapidly than methods involving external fixation. Because the drill site was adjacent to a readily identifiable anatomical landmark (the distal end of the tibial crest), it was easy to locate the lesion during microtomy. Thus, the mouse bone repair model described here satisfies all of the objectives of our study.

The process of bone repair in the model described here occurred primarily through the deposition of woven bone throughout the drill site, followed by modeling to remove bone from the marrow cavity and consolidate the new bone in the cortex. Expression of type III collagen, which is known to be upregulated during early fracture repair [9], was detectable in the drill site at day 5, and preceded expression of type I collagen. Type I collagen was homogeneously expressed throughout the drill site at day 7 when sparse islands of osteopontin staining and mineralization first appeared. The association of osteopontin expression with the mineralization phase of bone repair is in agreement with the observations of Yamazaki et al. [10], who investigated osteopontin transcript expression in a rat femoral fracture repair model. Trabeculae of well-mineralized woven bone, which stained strongly for the presence of type I collagen and osteopontin, were present throughout the drill site at day 9. Osteoclasts in the drill site were present at day 9, and in larger numbers at day 14, by which

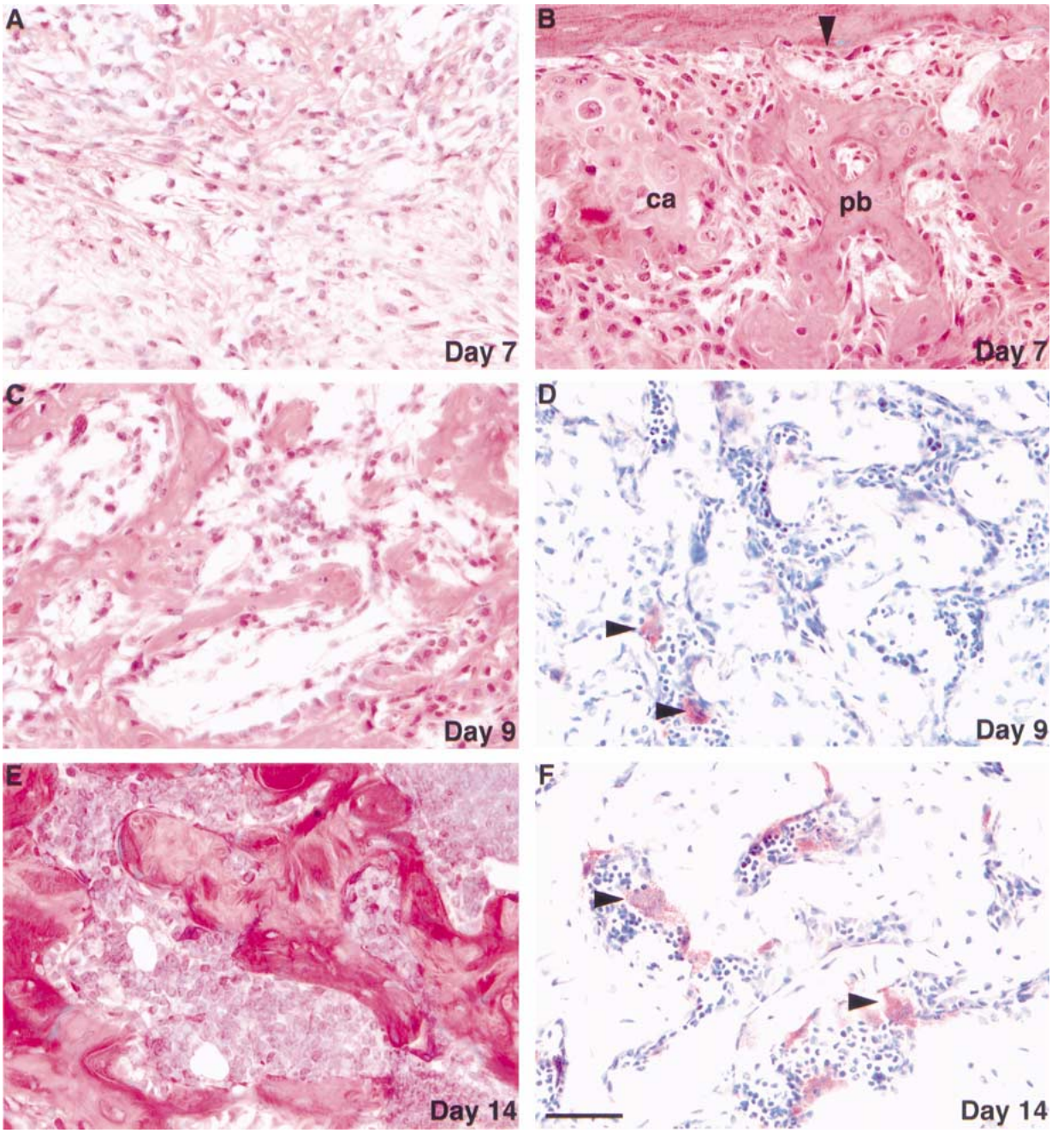

Fig. 3. Cellular composition of repair tissue. Transverse sections through the drill site (**A**, **C**–**F**) or adjacent periosteum (**B**), 7 (**A**, **B**), 9 (**C**, **D**) or 14 (**E**, **F**) days after drilling. Demineralized plastic sections stained with Masson's trichrome (**A**–**C**, **E**), and demineralized cryosections stained for the presence of TRAP and counterstained with hematoxylin (**D**, **F**). Arrowhead in **B** indicates the periosteal surface of preexisting cortical bone; ca – cartilage; pb – periosteal new bone. Arrowheads in **D** and **F** indicate TRAP-positive osteoclasts. Bar (**F**) represents 50 μm; the magnification is the same for all figure parts.

time significant modeling of bone had occurred in this location. Modeling continued until a relatively normal structure was achieved by 6 weeks after injury.

When the study described here was close to completion, descriptions of two models of trabecular bone repair in the mouse were published [11, 12]. One of these involves a drill hole in the third caudal vertebra, repair of which was analyzed by noninvasive imaging methods rather than histology [11]. The other method involves a defect in the femoral metaphysis induced by insertion of a wire to create a hole, followed by expansion of the hole manually using a drill bit, and the repair process has been analyzed histologically [12, 13]. Although this model investigates metaphyseal (trabecular) repair whereas ours involves diaphyseal (cortical) repair, there are some similarities between the two

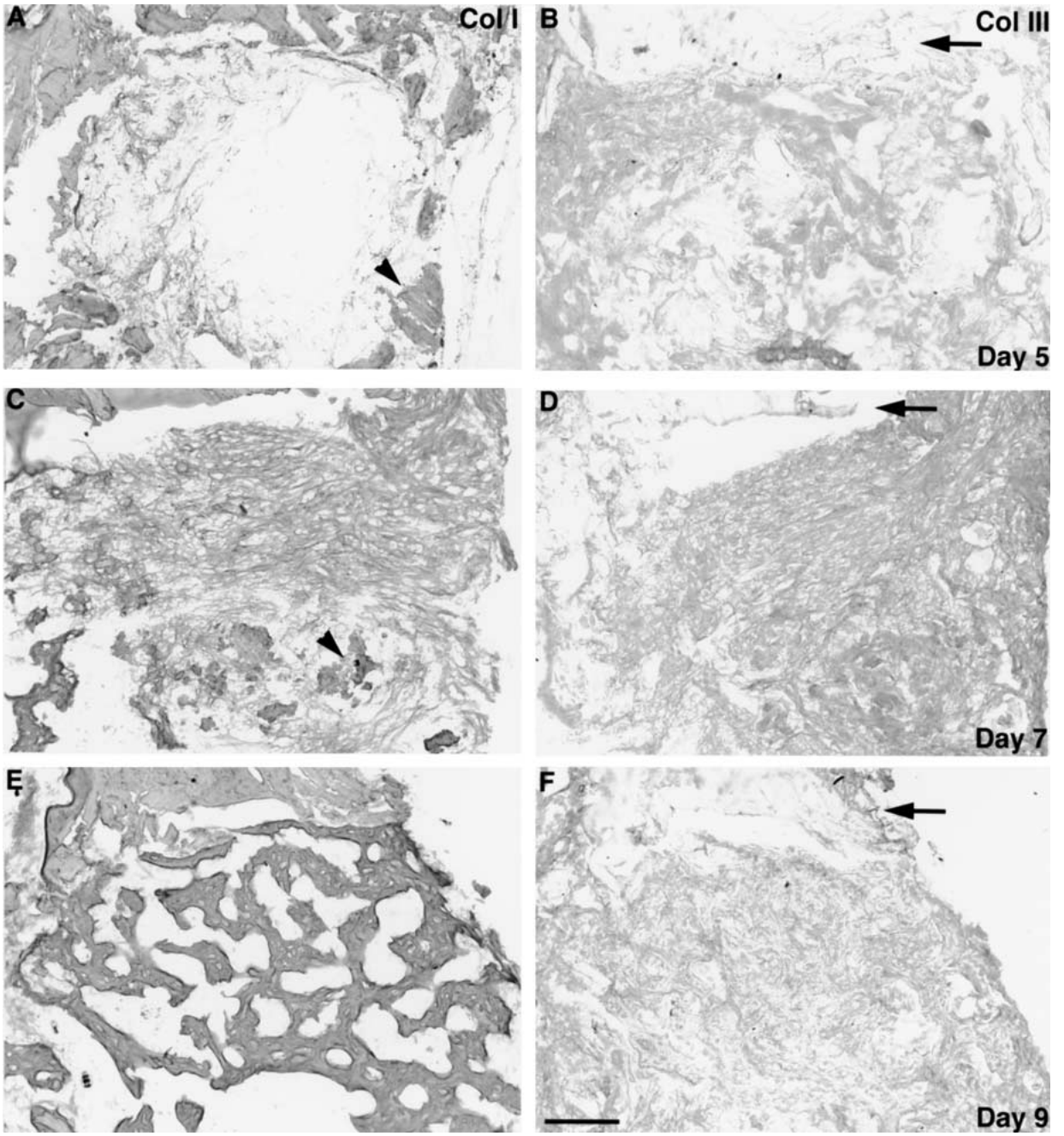

Fig. 4. Expression of type I and III collagen in repair tissue. Transverse sections of the tibia through the drill site 5 (**A**, **B**), 7 (**C**, **D**) or 9 (**E**, **F**) days after drilling. Adjacent demineralized cryosections stained for the presence of type I collagen (**A**, **C**, **E**) or type III collagen (**B**, **D**, **F**). Arrows indicate the edge of the drill site, and arrowheads indicate bone chips resulting from drilling. Images in this figure are rotated 90° clockwise with respect to those in Figure 1. Bar = 100 μm.

models. At day 7 in both models, the defect is filled with new woven bone, and small areas of cartilage are present on the adjacent periosteal surface. A return to virtually normal structure has been achieved within 6 weeks in both models.

The mouse model of cortical bone repair described here will provide a useful means of investigating this process in mice. The drill site provides a readily identifiable lesion of defined size and location, which undergoes an orderly and predictable series of events, leading to the return to normal tissue structure. This model will be of particular value in the investigation of bone repair in transgenic mice in which expression of proteins thought to be important in bone cell function has been manipulated.

Acknowledgments. This work was supported by the National Health and Medical Research Council of Australia, Project Grant No. 114140. The authors thank Su Toulson for excellent technical assistance.

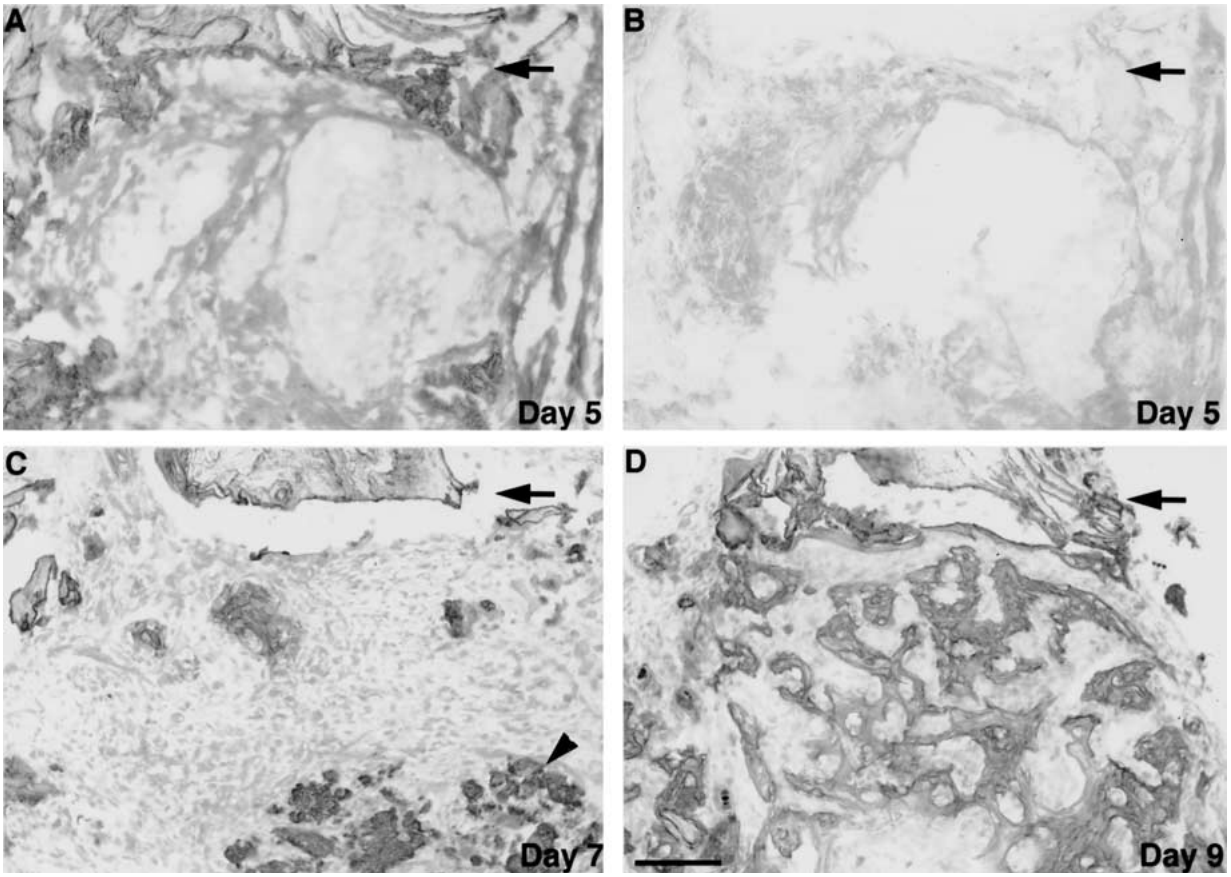

Fig. 5. Expression of osteopontin in repair tissue. Transverse sections of the tibia through the drill site 5 (**A**, **B**), 7 (**C**) or 9 (**D**) days after drilling. Demineralized cryosections stained with anti-osteopontin (**A**, **C**, **D**) or with normal rabbit serum (**B**). Arrows indicate the edge of the drill site, and arrowheads indicate bone chips resulting from drilling. Images in this figure are rotated 90° clockwise with respect to those in Figure 1. Bar = 100 μm.

References

1. Mackie EJ, Tucker RP (1999) The tenascin-C knockout revisited. J Cell Sci 112:3847–3853
2. Strandjord TP, Madtes DK, Weiss DJ, Sage EH (1999) Collagen accumulation is decreased in SPARC-null mice with bleomycin-induced pulmonary fibrosis. Am J Physiol 277:L628–635
3. Yoshitake H, Rittling SR, Denhardt DT, Noda M (1999) Osteopontin-deficient mice are resistant to ovariectomy-induced bone resorption. Proc Natl Acad Sci USA 96:8156–8160
4. Bourque WT, Gross M, Hall BK (1992) A reproducible method for producing and quantifying the stages of fracture repair. Lab Anim Sci 42:369–374
5. Hiltunen A, Vuorio E, Aro HT (1993) A standardized experimental fracture in the mouse tibia. J Orthop Res 11:305–312
6. Paccione MF, Warren SM, Spector JA, Greenwald JA, Bouletreau PJ, Longaker MT (2001) A mouse model of mandibular osteotomy healing. J Craniofac Surg 12:444–450
7. Li G, White G, Connolly C, Marsh D (2002) Cell proliferation and apoptosis during fracture healing. J Bone Miner Res 17:791–799
8. Mackie EJ, Ramsey S (1996) Expression of tenascin in joint-associated tissues during development and postnatal growth. J Anat 188:157–165
9. Page M, Hogg J, Ashhurst DE (1986) The effects of mechanical stability on the macromolecules of the connective tissue matrices produced during fracture healing. I. The collagens. Histochem J 18:251–265
10. Yamazaki M, Nakajima F, Ogasawara A et al. (1999) Spatial and temporal distribution of CD44 and osteopontin in fracture callus. J Bone Joint Surg Br 81:508–515
11. Li X, Gu W, Masinde G et al. (2001) Genetic variation in bone-regenerative capacity among inbred strains of mice. Bone 29:134–140
12. Uusitalo H, Rantakokko J, Ahonen M et al. (2001) A metaphyseal defect model of the femur for studies of murine bone healing. Bone 28:423–429
13. Eerola I, Uusitalo H, Aro H, Vuorio E (1998) Production of cartilage collagens during metaphyseal bone healing in the mouse. Matrix Biol 17:317–320